Available online at www.sciencedirect.com
SCIENCE DIRECT®
Journal of Chromatography A, 1043 (2004) 99–111
JOURNAL OF CHROMATOGRAPHY A
www.elsevier.com/locate/chroma

Selectivity differences in the separation of amphipathic α-helical peptides during reversed-phase liquid chromatography at pHs 2.0 and 7.0 Effects of different packings, mobile phase conditions and temperature

Y. Chen, C.T. Mant, R.S. Hodges*

Department of Biochemistry and Molecular Genetics, University of Colorado Health, Sciences Center, Denver, CO 80262, USA

Available online 24 May 2004

Abstract

In an ongoing effort to understand the effect of varying reversed-phase high-performance liquid chromatography (RP-HPLC) parameters on the retention behaviour of peptides, necessary for the rational development of separation/optimization protocols, we believe it is important to delineate the contribution of α-helical structure to the selectivity of peptide separations. The present study reports the effects of varying column packing, mobile phase conditions and temperature on RP-HPLC retention behaviour at pHs 2.0 and 7.0 of peptides based on the amphipathic peptide sequence Ac–EAEKAAKEXEKAAKEAEK–amide (with position X in the centre of the hydrophobic face of the α-helix), where position X is substituted by L- or D-amino acids. At pH 2.0, an increase in trifluoroacetic acid concentration or the addition of sodium perchlorate to a phosphoric acid-based mobile phase had the similar effect of improving peak shape as well as increasing peptide retention time due to ion-pairing effects with the positively-charged peptides; in contrast, at pH 7.0, the addition of salt had little effect save an improvement in peak shape. Temperature was shown to have a complex influence on peptide selectivity due to varying effects on peptide conformation. In addition, subtle effects on peptide selectivity were also noted based on the column packings employed at pHs 2.0 and 7.0.

Keywords: Selectivity; Mobile phase composition; Temperature effects; pH effects; Peptides

1. Introduction

The amphipathic α-helix is a very commonly encountered structural motif in peptides and proteins [1]. Approximately 50% of all helices in soluble globular proteins are amphipathic [1,2] with soluble proteins, by definition, having come to terms with an aqueous environment requiring burial of hydrophobic residues in the protein interior. Peptides that exhibit this structural motif have been extensively used as model systems to understand peptide or protein folding, stability and function [3–5]. For example, amphipathic helical structures are now known to play in important role in the mechanism of action of antimicrobial peptides, since the hydrophilic (positively charged) domain of the antimicrobial peptide initiates peptide interaction with the negatively charged bacterial phospholipids and the hydrophobic domain of the peptide would then permit the peptide to enter the membrane interior [6–9].

Reversed-phase high-performance liquid chromatography (RP-HPLC) is one of the most widely used techniques for the separation and purification of peptides and proteins [10,11]. Moreover, RP-HPLC also turns out to be a useful physicochemical probe for investigation of amphipathic helices induced or stabilized in hydrophobic environments [3,5,12–17]. For example, the hydrophobic interactions between polypeptides and the nonpolar stationary phase (typically aliphatic alkyl chains attached to a silica support) upon which RP-HPLC depends may well reflect similar intraprotein interactions between the nonpolar residues that stabilize the folded or three-dimensional structure of the native protein molecule [3]. In addition, the interaction of amphipathic α-helices with a hydrophobic surface during RP-HPLC is likely to be a good model for peptide binding to biological membranes or receptors [18–20]. In previous studies [5,12,21,22], we have stressed the importance of delineating the contribution of α-helical structure (both

* Corresponding author. Tel.: +1-303-315-8837; fax: +1-303-315-1153.
E-mail address: robert.hodges@uchsc.edu (R.S. Hodges).

0021-9673/$ – see front matter © 2004 Elsevier B.V. All rights reserved.
doi:10.1016/j.chroma.2004.04.028

amphipathic and non-amphipathic) to the selectivity of peptide separations, particularly since peptide fragments from chemical or proteolytic digests of proteins typically contain peptides with α-helical potential. With RP-HPLC applied to the separation of such peptide mixtures, any peptides with α-helical potential will be induced into such secondary structure by the non-polar environment characteristic of this technique (hydrophobic matrix and non-polar eluting solvent [12,15–17]).

In our aforementioned previous studies, we have (1) demonstrated the selectivity that may be obtained in a reversed-phase separation based on differences in peptide conformation (α-helical versus random coil) and highlighted by their retention time behaviour at varying gradients of organic modifier [21]; (2) we have utilized RP-HPLC to monitor the quantitative changes of apparent peptide side-chain hydrophobicity/hydrophilicity and peptide amphipathicity caused by single L- or D-amino acid substitutions in the centre of the hydrophobic face of a model amphipathic α-helical peptide [5]; and (3), we demonstrated interesting temperature selectivity effects in RP-HPLC due to conformation differences between non-helical and L- or D-amino acid substituted α-helical peptides [22]. In an ongoing effort to understand the effect of varying RP-HPLC parameters on the retention behaviour of peptides, necessary for the rational development of separation/optimization protocols, we report here the effects of varying column packing, mobile phase conditions and temperature on RP-HPLC retention behaviour at pHs 2.0 and 7.0 of peptides based on the amphipathic peptide sequence Ac–EAEKAAKEXEKAAKEAEK–amide (with position X in the centre of the hydrophobic face of the α-helix), where position X is substituted by L- or D-amino acids.

2. Experimental

2.1. Materials

t-Boc-protected (*tert*-butyloxycarbonyl) amino acids were purchased from Advanced ChemTech (Louisville, KY, USA). *o*-Benzotriazol-L-yl-*N*,*N*,*N*′,*N*′-tetramethyluronium hexafluorophosphate (HBTU) and 4-methylbenzhydrylamine resin hydrochloride salt (MBHA) (100–200 mesh) were obtained from Advanced ChemTech. Anisole and 1,2-ethanedithiol (EDT) were supplied by Aldrich (Oakville, Canada). Dimethylformamide (DMF) was obtained from Fisher-Biotech (Fair Lawn, NJ, USA). Trifluoroacetic acid (TFA) was obtained from Halocarbon Products (River Edge, NJ, USA) and diisopropylethylamine (DIEA) was obtained from Caledon (Georgetown, Canada). Orthophosphoric acid was purchased from Anachemia (Toronto, Canada). Sodium perchlorate was obtained from FisherBiotech. HPLC-grade acetonitrile was purchased from EM Science (Gibbstown, NJ, USA).

2.2. Peptide synthesis

Synthesis of the helical peptides, Ac–EAEKAAKEX$_{D/L}$-EKAAKEAEK–amide, was carried out by standard solid-phase synthesis methodology using *t*-Boc chemistry and MBHA resin (0.97 mmol/g) on an Applied Biosystems peptide synthesizer Model 430A (Foster City, CA, USA). The Boc-groups were removed at each cycle with 50% (v/v) TFA in dichloromethane. Coupling of amino acids was carried out with 0.45 mmol HBTU–0.8 mmol DIEA–DMF at each cycle, where the protected amino acid was activated for 5 min prior to addition to the resin and shaking for 30 min. Finally, the peptides were acetylated with acetic anhydride–DIEA–dichloromethane (10:20:70, v/v/v). The peptides were cleaved from the resin by treatment with HF (30 ml/g resin) containing 10% anisole and 2% 1,2-ethanedithiol at −5 to 0 °C for 1 h. The cleaved peptide-resin mixtures were washed with diethyl ether (3 × 25 ml) and the peptides extracted with neat acetonitrile (3 × 25 ml). The resulting peptide solutions were then lyophilized prior to purification.

2.3. Instrumentation

The crude peptides were purified by preparative RP-HPLC on a Varian Vista Series 5000 Liquid Chromatograph (Varian, Walnut Creek, CA, UA).

The analytical HPLC consisted of an HP 1100 liquid chromatograph (Hewlett-Packard, Avondale, PA, USA), coupled with an HP 1100 series diode array detector and thermostatted column compartment, HP Vectra XA computer and HP LaserJet 5 printer.

The correct primary ion molecular masses of peptides were confirmed by VG Quattro electrospray mass spectrometry (Fisons, Pointe-Claire, Canada).

Amino acid analyses of purified peptides were carried out on a Beckman Model 6300 amino acid analyzer (Beckman, San Ramon, CA, USA).

2.4. Columns and HPLC conditions

Crude peptides were purified on a semi-preparative Zorbax 300 SB-C_8 column (250 mm × 9.4 mm i.d.; 6.5-μm particle size, 300-Å pore size; Agilent Technologies, Brockville, Canada) with a linear AB gradient (0.2% acetonitrile/min) at a flow rate of 2 ml/min, where eluent A was 0.1% aq. TFA in water and B was 0.1% TFA in acetonitrile.

Analytical RP-HPLC was carried out on a Zorbax 300 SB-C_8 column (150 mm × 2.1 mm i.d.; 5 μm particle size; 300 Å pore size) and a Zorbax Eclipse XDB-C_8 column (150 mm × 2.1 mm i.d.; 5 μm; 300 Å) from Agilent Technologies, using a linear AB gradient (0.5% acetonitrile/min) at a flow-rate of 0.25 ml/min, at pH 2.0 and 7.0. Mobile phase systems used in this study were divided into two groups: at pH 7.0, eluent A was 20 mM aq. PO_4 containing 0, 10, 25, 50 or 100 mM $NaClO_4$ and eluent B was eluent A also

containing 50% (v/v) acetonitrile; at pH 2.0, eluent A was, 20 mM aq. H_3PO_4 or 20 mM aq. H_3PO_4 containing 100 mM $NaClO_4$ and eluent B was eluent A also containing 50% (v/v) acetonitrile. For an alternative pH 2.0 system, eluent A was 6, 10, 25, 50 or 100 mM aq. TFA and eluent B was the corresponding concentration of TFA in acetonitrile.

2.5. Calculation of resolution

Resolution (R_s), the measure of a column to separate chromatographic peaks, can be calculated through the equation:

$$R_s = \frac{1.176\Delta t_R}{W_1 + W_2}$$

where Δt_R is the difference in retention time between two peptide peaks (1 and 2) and W_1 and W_2 are their peak widths at half height [10]. This equation is satisfied if the units of retention time and peak width are the same, such as minutes.

2.6. Characterization of helical structure

The mean residue molar ellipticities of the peptide analogues were determined by circular dichroism (CD) spectroscopy, using a Jasco J-720 spectropolarimeter (Jasco, Easton, MD, USA), at 5 °C under benign conditions (50 mM aq. Phosphate–100 mM KCl, pH 7.0), as well as in the presence of an α-helix inducing solvent [23–25] 2,2,2-trifluoroethanol (TFE) (50 mM aq. Phosphate–100 mM KCl–50%TFE, pH 7.0). A 10-fold dilution of a ∼500 μM stock solution of the peptide analogues was loaded into a 0.02 cm fused silica cell and its ellipticity scanned from 190 to 250 nm. The values of molar ellipticities of the peptide analogues at wavelength 222 nm were used to determine the relative helicity of each peptide.

3. Results and discussion

3.1. Amphipathic α-helical model peptides

3.1.1. Design of model peptides

Our peptide models were designed based on the well-characterized sequence Ac–EAEKAAKEAEKAAKEAEK–amide, which exhibits a highly amphipathic α-helical structure (Fig. 1) and is denoted as peptide AA9 in previous studies [3,5,18–20,26–30]. In the design of this model peptide, alanine was selected to form the hydrophobic face of the helix because it contains the minimum side-chain hydrophobicity needed to create an amphipathic α-helix and because of its high intrinsic helical propensity and stability contributions [29–31]. Lysine and glutamic acid were also selected to allow a potential for α-helix stabilizing electrostatic attractions at the $i \rightarrow i+3$ and $i \rightarrow i+4$ positions at neutral pH values [32]. In order to reduce the unfavourable dipole interactions of α-helical structure, all substituted model peptides were synthesized with Nα-acetylated and Cα-amidated termini [33]. According to the study of Zhou et al. [29], this amphipathic α-helical model exhibits the following important features: (a) the helix is single-stranded and non-interacting, enabling the determination of the effect of different amino acid substitutions in the non-polar face; (b) there is a uniform environment created by alanine residues surrounding the substitution site in the centre of the non-polar face (position 9 of this 18-mer model peptide); (c) the small size of the alanine side-chain methyl group ensures the minimal interactions with the "guest" amino acid residues; (d) the relatively small size of the peptide (18 residues) maximizes the effects of single amino acid substitutions.

The Ala residue in the centre of the non-polar face of the amphipathic α-helical sequence of AA9 was substituted for the present study with L- or D-proline, L- or D-serine and L- or D-glutamine, or by glycine. The side chains of proline, serine and glutamine are uncharged at pHs 2.0 or 7.0, thus eliminating any chance of charge contributions of these substituted amino acids complicating interpretation of results. It should be noted that the intrinsic hydrophobicity of the non-polar face of the amphipathic α-helix is identical for each diastereomeric peptide pair. Since glycine does not exhibit optical activity, the Gly-substituted analogue represents a useful reference standard. Different α-helical peptide analogues were denoted by the one-letter code of the amino acid residue substituted at position 9 of the sequence (Fig. 1). For example, peptide P_D represents the model peptide analogue with D-proline substituted at position 9 and peptide G denotes the glycine-substituted analogue, etc.

Peptide C3 represents a peptide designed to exhibit negligible secondary structure, i.e., a random coil, although Fig. 1C (helical net) and Fig. 1D (helical wheel) present this peptide in the form it would take if it was able to become helical. This peptide was originally designed to be of the same length and similar composition to AA9, which may be viewed as the "native" peptide of the model amphipathic α-helical peptides. However, while AA9 contains seven Ala residues, C3 contains none (Fig. 1). With seven Ala residues in the hydrophobic face of AA9 (hence, seven CH_3 groups) and five Gly and two Leu residues in a putative hydrophobic face for C3 (hence eight CH_2 and CH_3 groups, from the two Leu residues), overall hydrophobicity is essentially maintained. The two additional Leu residues in the putative hydrophilic face in C3, if it were α-helical, were designed to increase the retention time of the random coil peptide and to ensure that it could not form an amphipathic α-helix. From Fig. 1D, it can be seen that, even if this peptide were able to be induced into α-helical structure, a non-amphipathic helix would result. However, the presence of five Gly residues, a well-known α-helix disrupter and, with the sole exception of proline, the amino acid with the lowest helical propensity [29,30], in place of five Ala residues was designed to make any secondary structure highly unlikely to occur. In addition, we have also shuffled the positions of positively-charged Lys and negatively-charged Glu residues to reduce further the possibility of intrachain electrostatic attractions, such as

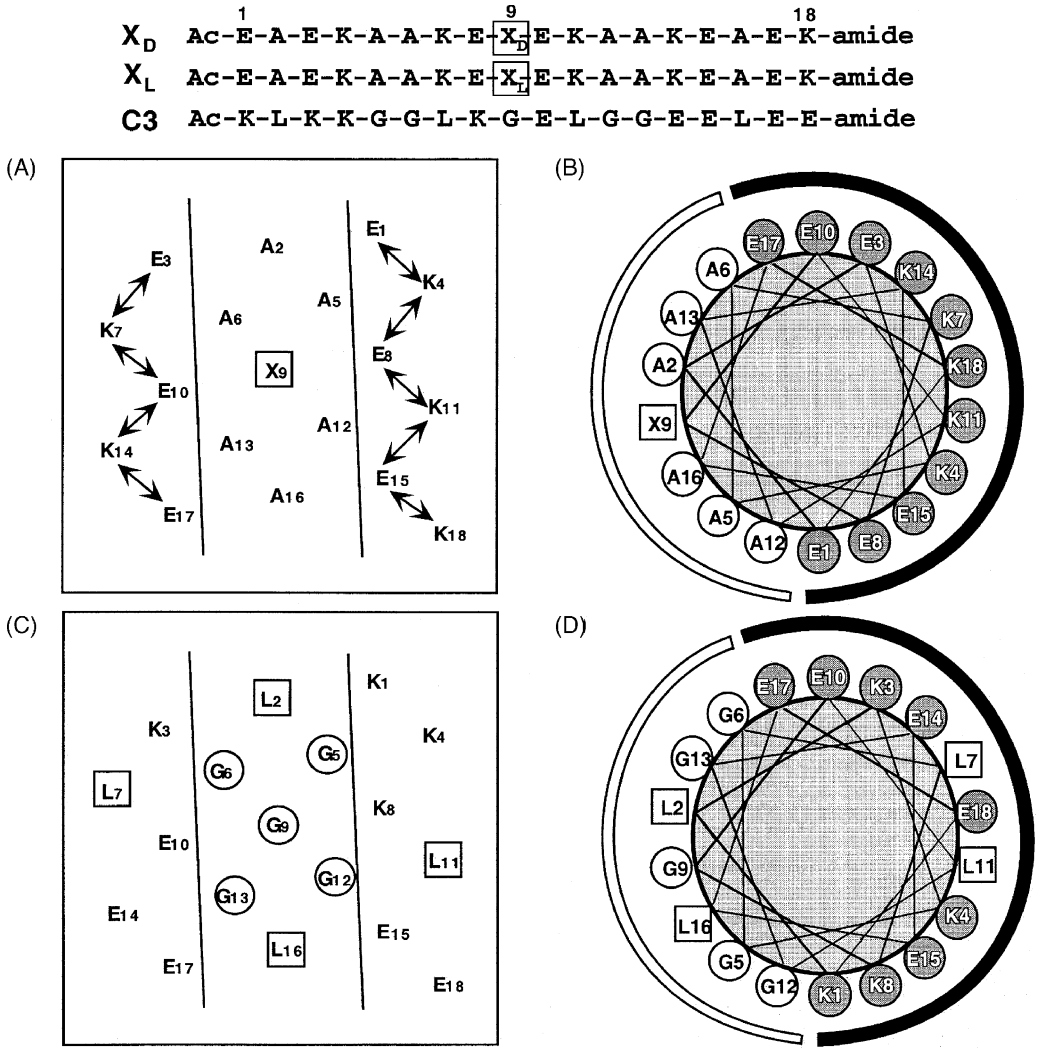

Fig. 1. (Top) Sequences of amphipathic α-helical peptides (X_D and X_L) and random coil peptide, C3, where X_D and X_L represent substituted D- and L-amino acids, respectively. (Bottom) Representations of the α-helical peptides as a helical net (A) and a helical wheel (B) and the random coil peptide, C3, as a helical net (C) and a helical wheel (D) if it were able to form an α-helix. The non-polar face of the amphipathic peptide sequence is indicated between two parallel lines in A and as an open arc in B; the hydrophilic face is shown as a solid arc in B. The substitution ("guest") site is at position 9 (boxed) of the non-polar face. The areas in the helical net representation (A) denote potential intrachain electrostatic interactions (attractions) at pH 7.0. Ac denotes Nα-acetyl and amide denotes Cα-amide. One-letter designations are used for the amino acid residues.

those able to stabilize the α-helical structure of AA9 (or other analogues) at pH 7.0 (compare Fig. 1A for the amphipathic α-helical analogues with Fig. 1C for putative helical structure of C3).

3.1.2. CD spectroscopy studies

In order to determine the effect of different substitutions on α-helical peptide conformation, CD spectra of the peptide analogues were measured under benign buffer conditions (50 mM PO_4, 100 mM KCl, pH 7.0) and also in the presence of the α-helix-inducing solvent TFE for all seven potentially α-helical analogues and for the reference standard C3.

From Fig. 2A, it can be seen that although peptide Q_L ($[\theta]_{222} = -13450^\circ$) exhibited considerably more α-helical structure than its diastereomer, peptide Q_D ($[\theta]_{222} = -2560^\circ$) in benign buffer, the molar ellipticity values of this diastereomeric peptide pair were very similar ($[\theta]_{222} = -27650^\circ$ and -24450° for peptides Q_L and Q_D, respectively, in the presence of 50% TFE. The helix-disrupting characteristics in benign medium of D-amino acid residues in peptide sequences otherwise made up solely of L-amino acids is well documented [5,34–37]; in addition, the attainment of high helicity of even such D-substituted peptides in the presence of TFE has also been demonstrated. Thus, from a previous study in our laboratory [5], all of the model peptide analogues, excluding the L-/D-proline substituted peptides, exhibited similar molar ellipticity values at 222 nm in the presence of 50% TFE, with >90% helical content. Since TFE is recognized as a useful mimic of the hydrophobic environment characteristic of RP-HPLC [12], as well as being a strong α-helix inducer in potentially helical molecules [23–25], elution of these peptide analogues

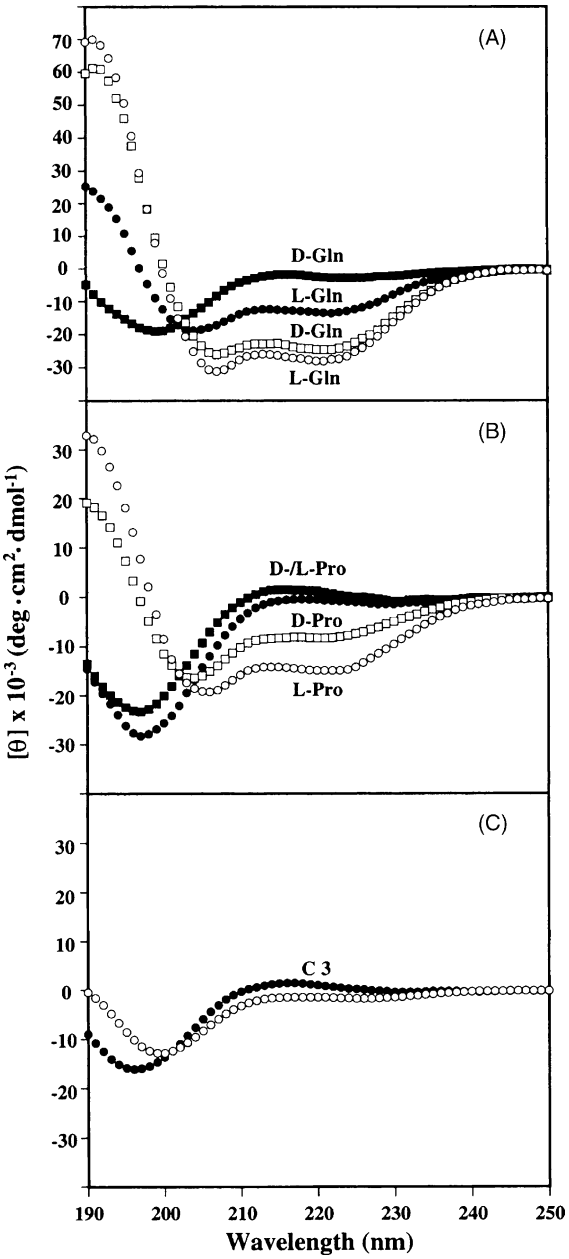

Fig. 2. Circular dichroism (CD) spectra of synthetic model peptides. Solid symbols represent CD spectra of peptide analogues obtained under benign conditions (i.e., in the absence of denaturant); open symbols represent spectra obtained in the presence of 50% (v/v) trifluoroethanol (TFE). (A) The results for Q_L and Q_D are denoted by circles and squares, respectively. (B) The results for P_L and P_D are denoted by circles and squares, respectively. The sequences of the model peptides and the random coil peptide, C3 (Panel C) are shown in Fig. 1 with denotions described in the text. CD conditions are described in Section 3.1.2.

as α-helices during RP-HPLC is ensured. In addition, the $[\theta]_{220}/[\theta]_{207}$ ratio values of Q_L and Q_D (and, indeed, S_L, S_D, and G) were less than 1.0 suggesting that, in the presence of 50% TFE, these peptides are single-stranded α-helices [24,27,28]. Hence, such observations also suggest that peptides Q_L, Q_D, S_L, S_D and G are eluted in a single-stranded α-helical conformation during RP-HPLC.

Both P_L and P_D exhibited molar ellipticities ($[\theta]_{222} = -700^\circ$ and 700°, respectively) characteristic of negligible secondary structure in benign medium (Fig. 2B). Even in the presence of 50% TFE, molar ellipticity values of just -14900° (P_L) and -8150° (P_D) were achieved, reflecting the strong helix-disrupting character of proline. Thus, with a Pro residue substituted into the centre of the non-polar face of the model helical peptide, ∼50% (P_L) or 75% (P_D) of the sequence could not be induced into α-helical structure in the presence of TFE, suggesting that these peptides will be eluted only with partial α-helical structure during RP-HPLC.

Finally, from Fig. 2C, peptide C3, designed as a random coil peptide standard, exhibited the expected negligible secondary structure in both benign buffer and in the presence of 50% TFE.

3.1.3. RP-HPLC elution behaviour of amphipathic α-helical peptides

It is well known that characteristic RP-HPLC conditions (hydrophobic stationary phase, non-polar eluting solvent) induce helical structure in potentially helical polypeptides [12,15–17]. Polypeptides, such as our model peptides (Fig. 1), which are thus induced into an amphipathic α-helix on interaction with a hydrophobic RP-HPLC stationary phase will exhibit preferred binding of their non-polar face with the stationary phase. Zhou et al. [12] clearly demonstrated that, because of this preferred binding domain, amphipathic α-helical peptides are considerably more retentive than non-amphipathic peptides of the same amino acid composition. From Fig. 1, as mentioned previously, the central substitution site of model peptide ensures intimate interaction of the substituting side-chain with the reversed-phase stationary phase; concomitantly, this is designed to maximize any observed effects on RP-HPLC retention behaviour of different amino acid substitutions at this site.

3.2. HPLC run parameters investigated in this study

3.2.1. Anionic ion-pairing reagents

Peptides are charged molecules at most pH values and the presence of different counterions will influence their chromatographic behaviour. The majority of researchers utilizing ion-pair RP-HPLC at low pH for the separation of peptide mixtures still take advantage of the excellent resolving power and selectivity of aq. TFA to TFA–acetonitrile gradients [10,11], although aq. H_3PO_4–acetonitrile systems have also shown their worth for peptide applications [10,11,21,38–40]. Favoured models for the mechanism of ion-pair separations involve either formation of ion pairs with the sample solute in solution followed by retention of the solute molecules on a reversed-phase column [41,42], or a dynamic ion-exchange event in which the ion-pairing reagent is first retained by the reversed-phase column and then solute molecules exchange ions with the counterion associated with the sorbed ion-pair reagent [42–45]. Whatever the mechanism, the resolving power of ion-pairing reagents is effected by interaction with

the ionized groups of a peptide. Anionic counterions such as trifluoroacetate (TFA^-) or phosphate ($H_2PO_4^-$) will interact with the protonated basic residues of a peptide (Lys, Arg, His or a free α-amino group). A hydrophobic counterion such as TFA^- will, though interaction with the positive groups in the peptide, increase further the affinity of the peptides for the hydrophobic stationary phase; in contrast, a polar hydrophilic counterion such as $H_2PO_4^-$, following ion-pair formation, will neutralize the positive charge on the peptides (thereby decreasing the peptide hydrophilicity) but would be unlikely to interact with the non-polar sorbent [40].

3.2.2. Salt additives to mobile phase

Addition of salts to mobile phases over a pH range of approximately 4–7 is traditionally designed to suppress negatively charged silanol interactions with positively charged solutes [10,11,39,46–50]. However, the potentially beneficial effect of salt, specifically $NaClO_4$, on peptide separations at low pH has also been demonstrated [50]. Indeed, the negatively charged perchlorate (ClO_4^-) ions acts as a hydrophilic anionic ion-pairing reagent and, thus, interacts with positively charged groups in a similar manner to $H_2PO_4^-$ and TFA^-. $NaClO_4$ is also particularly useful as the salt additive to a RP-HPLC mobile phase since it is highly soluble in aqueous acetonitrile eluents, even at relatively high concentrations of this organic modifier [51].

3.2.3. RP-HPLC stationary phases

Although optimization of peptide and protein separations during RP-HPLC has generally been achieved via manipulation of the mobile phase on a given reversed-phase column, the employment of different stationary phases, preferably with complementary selectivities, has also seen some success. Generally, for silica-based stationary phases, useful selectivity differences for peptides/proteins have been noted when the bonded-phase functionalities are significantly different, e.g., *n*-alkyl bonded-phase versus cyanopropyl and/or phenyl bonded phases [10,52–58], or long chain *n*-alkyl bonded-phases (C_8, C_{18}) versus shorter *n*-alkyl functionalities (C_3, C_4) [58].

In the present study, we wished to determine whether different columns containing an identical bonded-phase functionality would offer useful selectivity differences for our model amphipathic α-helical peptides under varying mobile phase conditions. As noted by Boyes and Walker [58], comparisons of bonded-phase mediated selectivity effects should be carried out using the same based silica support to minimize potential complications of varying silanol contributions to retention processes. Thus, the present study employed two C_8-bonded phases based on the same silica support and column dimensions (150 mm × 2.1 mm i.d.; 5-μm particle size; 300-Å pore size) from the same manufacturer: (1) Zorbax SB-300C_8 ("SB" denoting "StableBond"), prepared from monofunctional *n*-octylsilane and based on protecting the siloxane bond between the silica and the C_8 group with bulky side groups, in this case two isopropyl groups (monochlorodiisopropyl *n*-octylsilane) [58–61]; and (2) Zorbax XDB-C_8 ("XDB" denoting extra dense bonding), prepared by bonding a dense monolayer of dimethyl-*n*-octylsilane to the silica support, followed by exhaustive double endcapping with dimethyl- and trimethylsilane groups [62,63]. The SB packing was originally designed to protect the siloxane bond from acid hydrolysis at low pH, while the XDB packing was intended to shield the silica support from dissolution at pH values at neutrality and higher. In addition, both packings were also designed to exhibit thermal stability over a wide temperature range.

3.2.4. Temperature

Generally, the variation of temperature for RP-HPLC applications has implied raising the temperature in order to attempt improvement of solute separations. Since reversed-phase stationary phases with excellent thermal stability have now been commercially available for several years [58–63], the potential of this separation approach is now being realized, not least for resolution of peptide mixtures [22,64–66]. For instance, an interesting recent example by our laboratory [22] demonstrated that it is possible to manipulate polypeptide separations by subjecting mixtures of α-helical and random coil peptides to RP-HPLC at various temperatures (5–80 °C); depending on the stability of the individual components of secondary structure in the mixture, the molecules unfolded to different extents at different temperatures and, hence, interact with the stationary phase to differing extents, thus effecting a separation based on variations in peptide stability.

3.3. Effect of run parameters on RP-HPLC of amphipathic α-helical peptides

3.3.1. Effect of salt on RP-HPLC of model peptides at pHs 2.0 and 7.0

Fig. 3 shows the elution behaviour of the seven model peptides at pH 7.0 in the absence (Fig. 3A) and presence (Fig. 3B) of 100 mM $NaClO_4$ on the XDB-C_8 column. From Fig. 3 and Table 1, in both the absence and presence of salt, L-amino acid substituted peptides are consistently retained longer than their D-amino acid substituted counterparts; in addition, peptide elution order remains the same in the absence and presence of salt. The lesser retentiveness of the D-analogues compared to their L-enantiomers is likely due to disruption of the non-polar face of the amphipathic α-helix when introducing a D-amino acid into an α-helix otherwise made up of L-amino acids [5,35–37]; the apparent hydrophobicity of this preferred binding domain will thus be diminished relative to the amphipathic α-helix made up entirely of L-amino acids, resulting in the observed lower retention times of the D-amino acid substituted peptides of the L-/D-peptide pairs. It is interesting to note that P_L is eluted prior to both S_L and G, considering that Pro is considered to be a more hydrophobic residue than Ser or Gly [47]. However, since the presence of Pro severely disrupts the α-helix

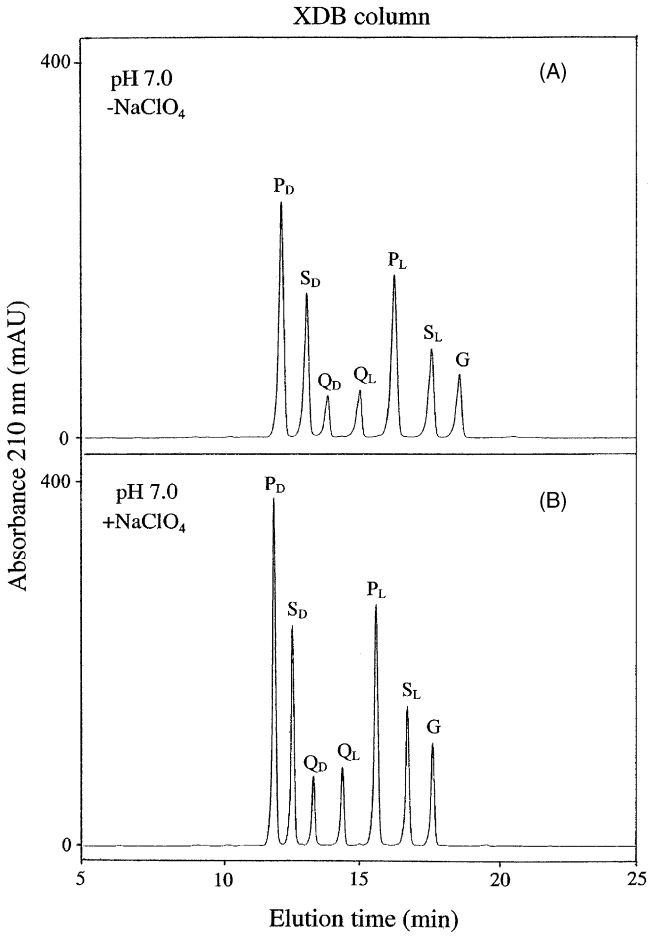

Fig. 3. Effect of salt on RP-HPLC elution profile of model peptides at pH 7.0. Conditions: (A) Linear AB gradient (0.5% CH_3CN/min) at a flow-rate of 0.25 ml/min, where eluent A is 20 mM aq. PO_4, pH 7.0, and eluent B is eluent A containing 50% CH_3CN; (B) same as (A) except for the addition of 100 mM $NaClO_4$ to both eluents; temperature, 65 °C.

(Fig. 2), with only ∼50% of P_L able to be induced into an α-helical structure, its concomitant severe disruption of P_L amphipathicity (and, hence, non-polar face) would result in a lesser retention time compared to the fully folded S_L and G analogues, despite the relatively lesser hydrophobicity of these two residues compared to Pro. A similar, albeit even more dramatic, observation was made for P_D (only ∼25% able to be induced into α-helical structure; Fig. 2), which was eluted prior to all peptide analogues.

From Fig. 3, there is a small reduction in retention time of all peptides in the presence of salt (Fig. 3B) compared to its absence (Fig. 3A), concomitant with decreasing peak widths ($W_{1/2}$) (Fig. 3; Table 1), this decrease in $W_{1/2}$ values also resulting in an increase in resolution (Rs) between adjacent peptides (Fig. 3; Table 2).

As noted above, the addition of salt above pH 4 is frequently necessary to block non-specific interactions between underivatized, negatively charged silanol groups on the silica support and positively charged residues, such interactions resulting in longer retention times and peak broadening. However, it is a testament to the dense bonded phase of this XDB, concomitant with the exhaustive end-capping during its production, that the peptide elution profiles in both the absence (Fig. 3A) and presence (Fig. 3B) of $NaClO_4$ were quite similar.

Table 1
Effect of $NaClO_4$ on peptide retention time and peak width during RP-HPLC at pH 7.0[a]

Peptides[b]	$t_{R(-NaClO_4)}$ (min)[c]	$t_{R(+NaClO_4)}$ (min)[c]	$W_{1/2(-NaClO_4)}$ (min)[d]	$W_{1/2(+NaClO_4)}$ (min)[d]
P_D	12.20	11.93	0.1744	0.1301
S_D	13.11	12.61	0.1749	0.1261
Q_D	13.86	13.36	0.1739	0.1202
Q_L	15.02	14.41	0.1822	0.1251
P_L	16.28	15.62	0.2049	0.1519
S_L	17.63	16.76	0.1935	0.1366
G	18.64	17.67	0.1935	0.1353

[a] Conditions: RP-HPLC at pH 7.0 on XDB-C_8 column (see Fig. 3).
[b] For peptide denotions, see Section 3.1.1.
[c] Denotes the retention times of the peptides during RP-HPLC at pH 7.0 with (+) or without (−) 100 mM $NaClO_4$.
[d] Denotes the peak width at half height of the peptides (in time units) during RP-HPLC at pH 7.0 with (+) or without (−) 100 mM $NaClO_4$.

Fig. 4 shows the elution behaviour of the seven model peptides at pH 2.0 under mobile phase conditions employing 20 mM H_3PO_4 in the absence (Fig. 4A) or presence (Fig. 4B) of 100 mM $NaClO_4$, 6 mM TFA (Fig. 4C) and 50 mM TFA (Fig. 4D). In contrast to results obtained at pH 7.0 (Fig. 3; Table 1), the retention times of all seven peptide analogues increased considerably in the presence of salt at pH 2.0 (Fig. 4B) compared to its absence (Fig. 4A). With the exception of the now coeluted Q_D/P_L, the resolution of adjacent peptide pairs improved in the presence of salt (Fig. 4B; Table 3) due, in a similar manner to the effect of salt at pH 7.0 (Fig. 3B; Tables 1 and 2), the decreasing $W_{1/2}$ values compared to its absence (Fig. 4A). Interestingly, increasing the concentration of TFA from 6 mM (Fig. 4C) to 50 mM

Table 2
Effect of $NaClO_4$ on peptide resolution during RP-HPLC at pH 7.0[a]

Peptide pair[b]	$\Delta t_{R(-NaClO_4)}$ (min)[c]	$\Delta t_{R(+NaClO_4)}$ (min)[c]	$R_{S(-NaClO_4)}$[d]	$R_{S(+NaClO_4)}$[d]
S_D–P_D	0.91	0.68	3.06	3.12
Q_D–S_D	0.75	0.75	2.53	3.58
Q_L–Q_D	1.16	1.05	3.83	5.03
P_L–Q_L	1.26	1.21	3.83	5.14
S_L–P_L	1.35	1.14	3.98	4.65
G–S_L	1.01	0.91	3.07	3.94

[a] Conditions: RP-HPLC at pH 7.0 on XDB-C_8 column (see Fig. 3).
[b] Denotes the later eluted peptide minus the adjacent earlier eluted peptide on the chromatogram in Fig. 3; for peptide denotions, see Section 3.1.1.
[c] Denotes the difference in retention time between two adjacent peptides in the same peptide pair during RP-HPLC at pH 7.0, with (+) or without (−) 100 mM $NaClO_4$; $\Delta t_R = t_R$ of former peptide minus t_R of adjacent earlier eluted peptide.
[d] Denotes the resolution of every two adjacent peaks during RP-HPLC at pH 7.0 with (+) or without (−) 100 mM $NaClO_4$.

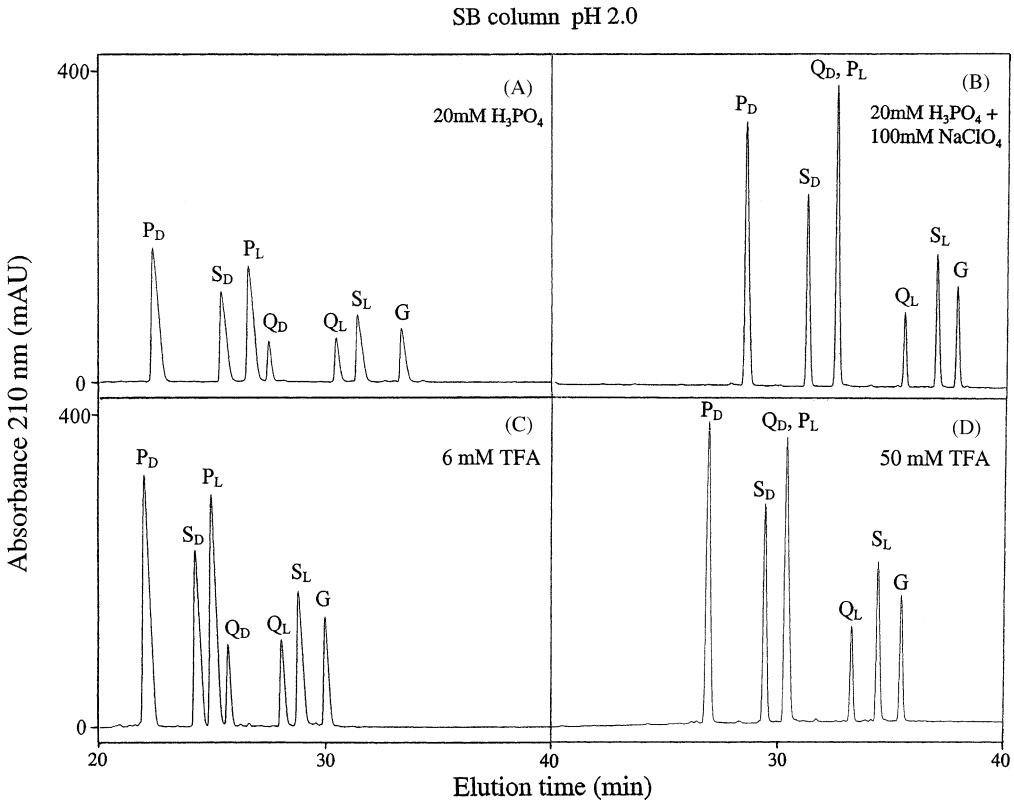

Fig. 4. Effect of mobile phase conditions on RP-HPLC elution profile of model peptides at pH 2.0. Conditions: all runs carried out with a linear AB gradient (0.5% CH_3CN/min) at a flow-rate of 0.25 ml/min; (A) eluent A is 20 mM aq. H_3PO_4, pH 2.0, and eluent B is eluent A containing 50% CH_3CN; (B) same as (A) except for the addition of 100 mM $NaClO_4$ to both eluents; (C) eluent A is 6 mM aq. TFA and eluent B is 6 mM TFA in CH_3CN; (D) eluent A is 50 mM aq. TFA and eluent B is 50 mM TFA in CH_3CN; temperature, 65 °C.

(Fig. 4D) had a similar effect to that of salt addition, i.e., an increase in peptide retention times concomitant with an increase in resolution between adjacent peptides (Table 3), mainly due again to a decrease in $W_{1/2}$ at the higher TFA concentration. Note also that Q_D and P_L are again coeluted in the presence of 50 mM TFA (Fig. 4D) in a similar manner to the presence of 100 mM $NaClO_4$ (Fig. 4B). An increase in retention time of positively charged peptides with increasing TFA concentration has been previously demonstrated [40].

The explanation for the increase in peptide retention times in the presence of salt (Fig. 4B) compared to its absence (Fig. 4A) is likely due to ion-pairing of the five basic, positively charged lysine residues with the negatively charged ClO_4^- anion, neutralizing the hydrophilic, charged character of the lysine side-chains and concomitantly enhancing

Table 3
Effect of eluent system on peptide resolution during RP-HPLC at pH 2.0[a]

Peptide pair[b]	20 mM H_3PO_4[c]		20 mM H_3PO_4–100 mM $NaClO_4$[c]		6 mM TFA[c]		50 mM TFA[c]	
	Δt_R (min)[d]	R_S[e]	Δt_R (min)[d]	R_S[e]	Δt_R (min)[d]	R_S[e]	Δt_R (min)[d]	R_S[e]
S_D–P_D	2.97	5.09	2.69	7.59	2.21	3.75	2.50	7.28
P_L–S_D	1.18	2.06	1.29	4.20	0.70	1.26	0.95	2.52
Q_D–P_L	0.87	1.72	–[f]	–[f]	0.70	1.42	–[f]	–[f]
Q_L–Q_D	3.00	6.86	2.99	9.59	2.38	5.97	2.87	7.46
S_L–Q_L	0.96	1.90	1.43	4.63	0.76	1.58	1.14	3.48
G–S_L	1.94	3.65	0.89	2.77	1.17	2.35	1.01	3.22

[a] Conditions: RP-HPLC at pH 2.0 on SB-C_8 column (see Fig. 4).
[b] Denotes the later eluted peptide minus the adjacent earlier eluted peptide on the chromatogram in Fig. 4; for peptide denotions, see Section 3.1.1.
[c] Denotes the different eluent systems as shown in Fig. 4.
[d] Denotes the difference in retention time between two adjacent peptides (peptide pair) in the corresponding eluent systems during RP-HPLC at pH 2.0; $\Delta t_R = t_R$ of peptide minus t_R of adjacent earlier eluted peptide.
[e] Denotes the resolution of every two adjacent peaks (peptide pair) in the corresponding eluent systems during RP-HPLC at pH 2.0.
[f] Dashes denote the coeluted peptides.

the hydrophobicity of the peptides. Support for this view, rather than an induction of hydrophobic interactions with the reversed-phase packing in the presence of 100 mM $NaClO_4$, also lies in the similar effect of increasing the concentration of TFA from 6 mM (Fig. 4C) to 50 mM (Fig. 4D). Note that the selectivity of the peptide separations effected by the ClO_4^- or TFA^- anions were the same.

A point of significance from Fig. 4 also lies in the relative effectiveness of the ClO_4^- and TFA^- anions in increasing peptide retention time with increasing anion concentration, i.e., an increase in TFA^- concentration of just 44 mM (50 mM in Fig. 4D minus 6 mM TFA in Fig. 4C) has a similar effect as the addition of 100 mM ClO_4^- (Fig. 4B) compared to its absence (Fig. 4A). This result is likely due to the aforementioned relative hydrophilic/hydrophobic properties of these anions. Thus, the presence of the hydrophilic ClO_4^- counterion simply reduces the hydrophilicity of the peptides via ion-pairing with the positively charged residues, thus increasing peptide retention time; in contrast, the hydrophobic TFA^- counterion not only reduces the hydrophilicity of the peptides through such ion-pairing but also further increases peptide hydrophobicity due to the hydrophobic nature of the TFA^- anion. Hence, a lower concentration of TFA will have a similar effect on peptide retention time as a significantly higher (about double, in this instance) concentration of $NaClO_4$.

At pH 2.0 (Fig. 4), the glutamic acid residues are uncharged and the peptides have a net charge of +5. However, at pH 7.0 (Fig. 3), both the lysine and glutamic acid residues are charged, producing an overall −1 charge on the peptides. Thus, the observation that the retention times of the peptides do not increase on the addition of salt at pH 7.0 (Fig. 3) can be explained on the basis of overall net charge. In addition, these results at pH 7.0 (Fig. 3), with no increase in peptide retention times in the presence of salt, also again suggests that induction of hydrophobic interactions with the column packing by the inclusion of 100 mM $NaClO_4$ is not a factor.

Fig. 5 illustrates graphically the effect of concentration of anionic ion-pairing reagents on peptide retention time at both pH 2.0 (Fig. 5A, TFA^- anion; Fig. 5B, ClO_4^- anion) and pH 7.0 (Fig. 5C, ClO_4^- anion). From Fig. 5, the similar effect of TFA^- (5A) and ClO_4^- (5B) is quite clear, i.e., an increase in retention time of the α-helical peptides with increasing anion concentration. In addition, an increase in salt concentration at pH 7.0 (Fig. 5C) is again (see Fig. 3) seen to have negligible effect on peptide retention time.

A significant result from Fig. 5 is the similarity of the profile for the random coil peptide, C3, compared to those of the α-helical peptides. At pH 7.0, a fully folded α-helical peptide would allow intrachain electrostatic interactions between lysine and glutamic acid residues. Potentially, the negligible effect of ClO_4^- at pH 7.0 could be viewed as an inability to compete with the negatively charged glutamic acid residues for ion-pairing with the lysine side-chains, i.e., a conformational aspect to the differences in peptide elution behaviour at pH 2.0 versus pH 7.0 rather than simply

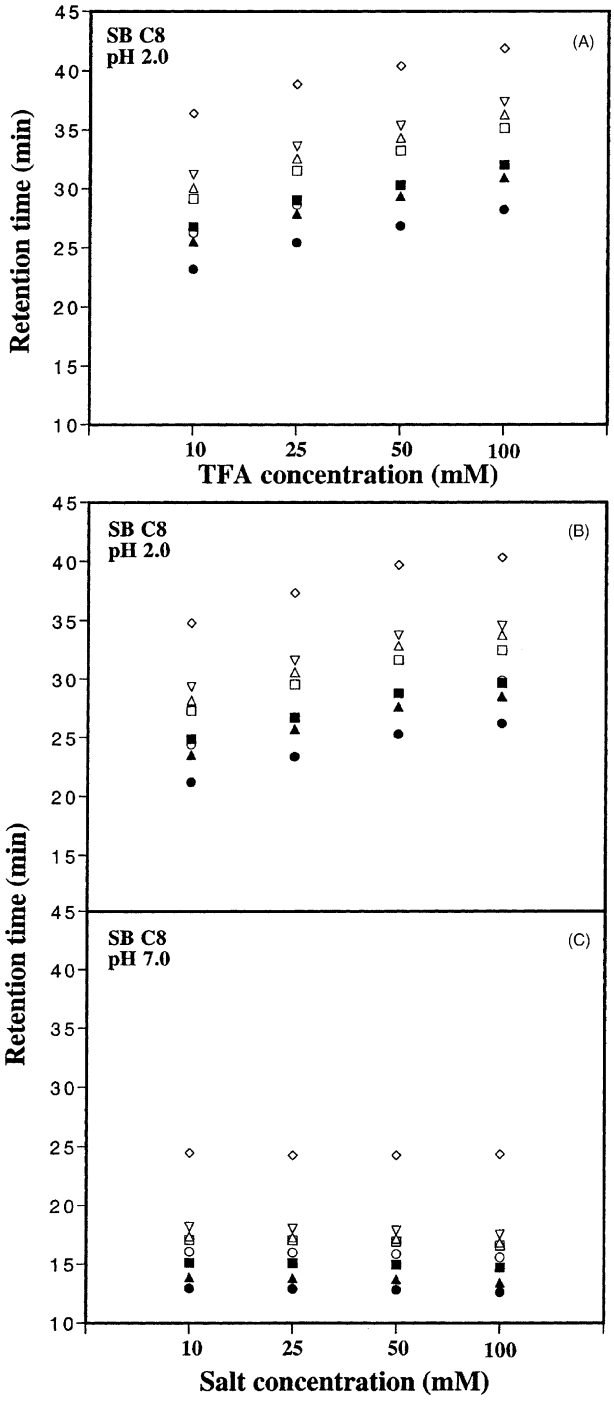

Fig. 5. Effect of concentration of anionic ion-pairing reagents on the retention time of model peptides at pHs 2.0 and 7.0. Conditions: linear AB gradient (0.5% CH_3CN/min) at a flow-rate of 0.25 ml/min for all runs; (A) eluent A is 10, 25, 50 or 100 mM aq. TFA and eluent B is the corresponding TFA concentration in CH_3CN; (B) eluent A is 10, 25, 50 or 100 mM $NaClO_4$ in 20 mM aq. H_3PO_4, pH 2.0, and eluent B is the corresponding eluent A containing 50% CH_3CN; (C) eluent A is 10, 25, 50 or 100 mM $NaClO_4$ in 20 mM aq. PO_4, pH 7.0, and eluent B is the corresponding eluent A containing 50% CH_3CN; temperature, 65 °C. Symbols used are open diamonds for random coil peptide C3, open inverted triangles for G, open upright triangles for S_L, closed upright triangles for S_D, open squares for Q_L, closed square for Q_D, open circle for P_L and closed circles for P_D.

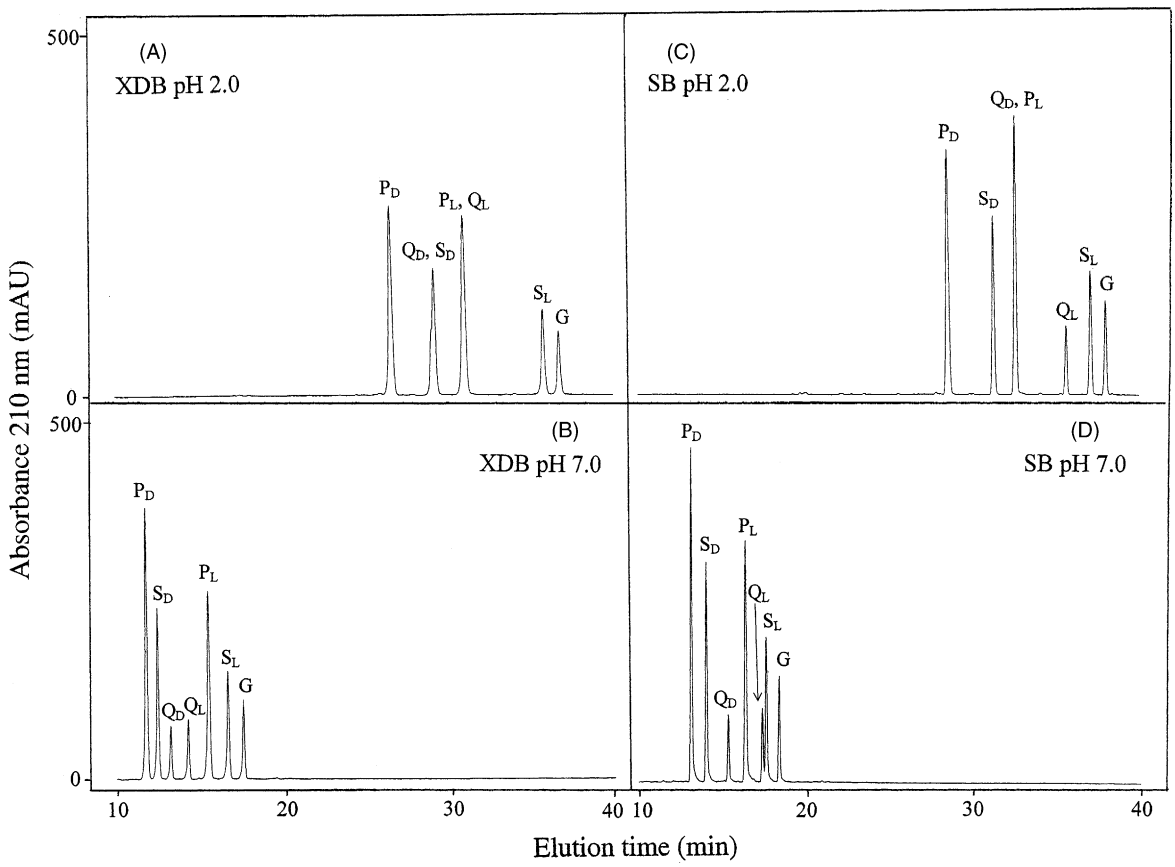

Fig. 6. Comparison of RP-HPLC retention behaviour on XDB and SB-C_8 columns at pH 2.0 and pH 7.0. Conditions: all runs were carried out by linear gradient elution (0.5% CH_3CN/min) at a flow-rate of 0.25 ml/min; (A and C) eluent A is 20 mM aq. H_3PO_4, pH 2.0, and eluent B is eluent A containing 50% CH_3CN, both eluents containing 100 mM $NaClO_4$; (B and D) eluent A is 20 mM aq. PO_4, pH 7.0, and eluent B is eluent A containing 50% CH_3CN, both eluents containing 100 mM $NaClO_4$, temperature, 65 °C.

a matter of overall net charge (+5 and −1, respectively). However, the random coil C3 is unable to exhibit such intrachain interactions; indeed, P_L and (particularly) P_D would also be limited in this respect. Thus, the observation that the random coil C3, the partially folded P_L and P_D and the fully folded G, S_L, S_D, Q_L and Q_D all exhibited similar responses to increases in perchlorate concentration at both pH 2.0 and pH 7.0 indicates that counterion concentration effects are *conformation independent.*

3.3.2. Effect of column packing on RP-HPLC of model peptides at pHs 2.0 and 7.0

Fig. 6 compares the retention behaviour of the α-helical peptides on the XDB (Fig. 6A and B; pHs 2.0 and 7.0, respectively) and SB (Fig. 6C and D; pHs 2.0 and 7.0, respectively) C_8 columns. From Fig. 6B, selectivity differences between the two column packings are apparent both at pH 2.0 (panels A and C) and pH 7.0 (panels B and D). Thus, at pH 2.0, there is considerable movement of Q_D and Q_L relative to the other peptides between the two columns: Q_D/S_D and P_L/Q_L are coeluted peptide pairs on the XDB column (Fig. 6A), while Q_D/P_L is a coeluted pair on the SB column (Fig. 6C). At pH 7.0, Q_L is eluted prior to P_L on the XDB column (Fig. 6B) and after P_L on the SB column (Fig. 6D). Further, for this peptide mixture, pH 7.0 resulted in better resolution of all six peptides in both columns compared to pH 2.0.

All peptides are eluted considerably earlier on both columns at pH 7.0 compared to pH 2.0. As noted previously for Fig. 4, the sodium perchlorate (specifically, the ClO_4^- anion) is able to act as an ion-pairing reagent at pH 2.0 since the peptides have an overall +5 net charge. In contrast, at pH 7.0, the overall net charge on the peptides is −1; thus, the salt is able to mask any unfavourable electrostatic interactions between the peptides and the hydrophobic stationary phase at this pH but does not act as an ion-pairing reagent, i.e., the charged character of the peptides makes them more hydrophilic at pH 7.0 compared to pH 2.0 where ion-pairing can take place.

3.3.3. Effect of temperature on RP-HPLC of model peptides at pHs 2.0 and 7.0

Fig. 7 illustrates the effect of temperature on elution behaviour of the α-helical peptides at pH 2.0 on the SB-C_8 column (designed, as noted previously, to exhibit excellent stability at acidic pH values [59–61]). From Fig. 7,

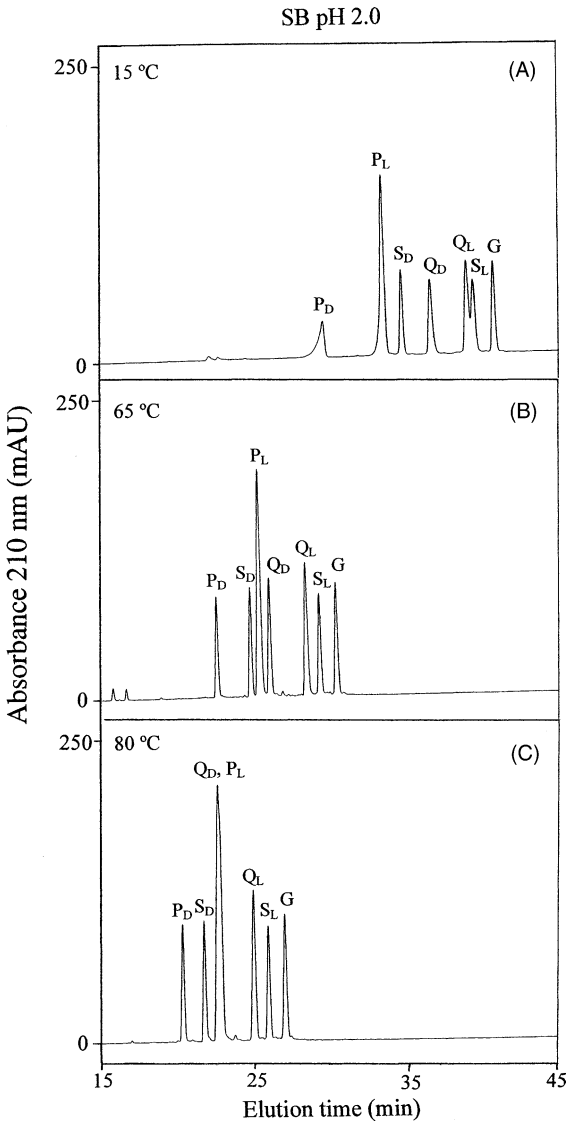

Fig. 7. Effect of temperature on RP-HPLC elution profile of model peptides at pH 2.0. Conditions, linear AB gradient (0.5% CH_3CN/min) at a flow-rate of 0.25 ml/min, where eluent A is 0.05% aq. TFA, pH 2.0, and eluent B is 0.05% aq. TFA in CH_3CN; temperature, 15 °C (A), 65 °C (B) and 80 °C (C).

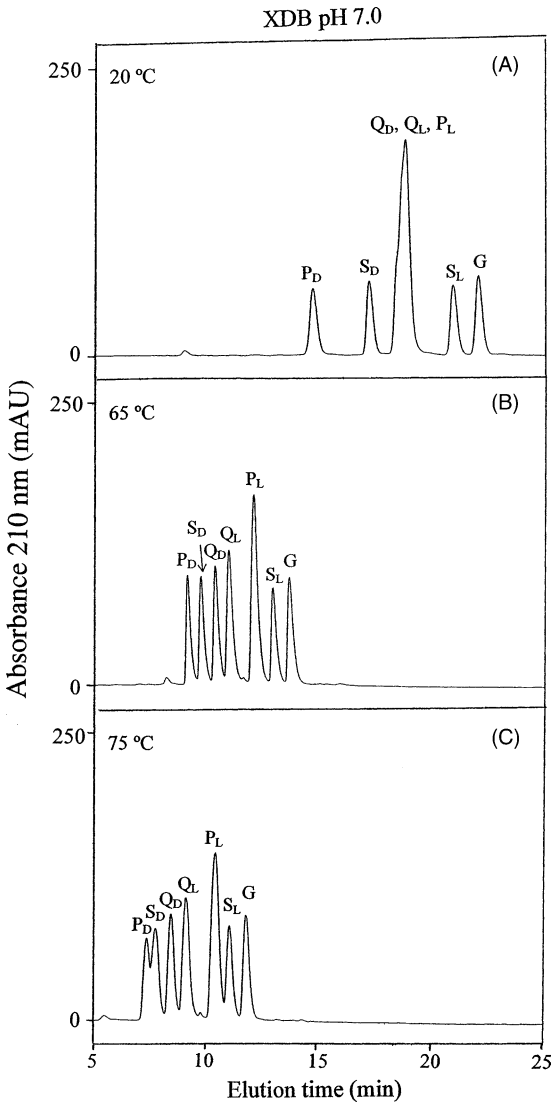

Fig. 8. Effect of temperature on RPC elution profile of model peptides at pH 7.0. Conditions, linear AB gradient (0.5% CH_3CN/min) at a flow-rate of 0.25 ml/min, where eluent A is 20 mM aq. PO_4, pH 7.0, and eluent B is eluent A containing 50% CH_3CN, both eluents containing 100 mM $NaClO_4$; temperature, 20 °C (A), 65 °C (B) and 80 °C (C).

increasing temperature both reduces peptide retention time and decreases peak widths, due to an enhancement of the mass-transfer rate of the peptide solutes between the mobile and stationary phases (a higher mass-transfer rate will reduce peak broadening and, hence, increase efficiency) [61,67–69]. For this peptide mixture, optimum resolution was obtained at 65 °C (Fig. 7B; Table 4), with Q_D and P_L being coeluted at 80 °C (Fig. 7C; Table 4).

The major selectivity changes with increasing temperature at pH 2.0 arise mainly from the behaviour of P_D and P_L which decrease in retention time less with increasing temperature relative to the other peptides. This is likely due to the different conformation-dependent responses of the peptides with temperature [70,71], with unfolding of the amphipathic peptides (and, hence, disruption of the preferred binding domain, i.e., the non-polar face) in solution as the temperature is raised, thus leading to a decrease in retention time (an average drop in t_R for the α-helical peptides of ∼14 min between 15 and 80 °C). In contrast, P_D and P_L (an average drop in t_R for P_D and P_L of ∼8 and 10 min, respectively, between 15 and 80 °C) are already 75% (P_D) or 50% (P_L) in a random coil configuration, even at low temperature; hence, their response to a temperature increase would not be as marked as that of a fully folded peptide analogue [70].

Fig. 8 now illustrates the effect of temperature on elution behaviour of the α-helical peptides at pH 7.0 on the XDB-C_8 column (designed, as noted previously, to exhibit excellent stability at neutral and higher pH values [62,63]).

Table 4
Effect of temperature on peptide resolution during RP-HPLC at pH 2.0[a]

Peptide pair[b]	Temperature (°C)[c]					
	15		65		80	
	Δt_R (min)[d]	R_S[e]	Δt_R (min)[d]	R_S[e]	Δt_R (min)[d]	R_S[e]
S_D–P_D	5.15	9.52	2.20	6.79	1.39	4.11
P_L–S_D	−1.24[f]	2.87	0.52	1.35	0.87	1.68
Q_D–P_L	3.14	6.37	0.73	1.79	–[g]	–[g]
Q_L–Q_D	2.35	4.81	2.37	6.26	2.34	4.27
S_L–Q_L	0.42	0.88	0.89	2.33	0.99	2.51
G–S_L	1.31	3.00	1.10	2.94	1.09	2.81

[a] Conditions: RP-HPLC at pH 2.0 on SB-C_8 column (see Fig. 7).
[b] Denotes the later eluted peptide minus the adjacent earlier eluted peptide on the chromatogram in Fig. 7; for peptide denotions, see Section 3.1.1.
[c] Chromatograms at the different temperatures are shown in Fig. 7.
[d] Denotes the difference in retention time between two adjacent peptides (peptide pair) at the corresponding temperature during RP-HPLC at pH 2.0, $\Delta t_R = t_R$ of peptide minus t_R of adjacent earlier eluted peptide.
[e] Denotes the resolution of every two adjacent peaks (peptide pair) at the corresponding temperature during RP-HPLC at pH 2.0.
[f] At 15 °C P_L is eluted prior to S_D.
[g] Dashes denote coeluted peptides.

Table 5
Effect of temperature on peptide resolution during RP-HPLC at pH 7.0[a]

Peptide pair[b]	Temperature (°C)[c]					
	20		65		75	
	Δt_R (min)[d]	R_S	Δt_R (min)[d]	R_S[e]	Δt_R (min)[d]	R_S[e]
S_D–P_D	2.50	4.23	0.59	1.52	0.39	0.75
Q_D–S_D	1.60	2.15	0.63	1.54	0.68	1.22
Q_L–Q_D	–[f]	–	0.61	1.34	0.66	1.13
P_L–Q_L	–	–	1.10	2.15	1.29	1.99
S_L–P_L	2.12	2.83	0.86	1.80	0.65	1.10
G–S_L	1.10	1.90	0.74	1.63	0.73	1.38

[a] Conditions: RP-HPLC at pH 7.0 on XDB-C_8 column (see Fig. 8).
[b] Denotes the later eluted peptide minus the adjacent earlier eluted peptide on the chromatogram in Fig. 8; for peptide denotions, see Section 3.1.1.
[c] Chromatograms at the different temperatures are shown in Fig. 8.
[d] Denotes the difference in retention time between two adjacent peptides (peptide pair) at the corresponding temperature during RP-HPLC at pH 7.0, $\Delta t_R = t_R$ of peptide minus t_R of adjacent earlier eluted peptide.
[e] Denotes the resolution of every two adjacent peaks (peptide pair) at the corresponding temperature during RP-HPLC at pH 7.0.
[f] Dashes denote coeluted peptides.

From Fig. 8, in a similar manner to pH 2.0 (Fig. 7), increasing temperature decreases peptide retention time. Peak width also generally decreases with increasing temperature, with optimum resolution of the peptide mixture, in a similar manner to the pH 2.0 results (Fig. 7; Table 4) being obtained at 65 °C (Fig. 8B; Table 5). Note that the broader peaks and reduced retention times of the peptides in Fig. 8B compared to Fig. 6B, where the same column and conditions were used, is likely due to column aging in the former. Between 20 and 75 °C (Fig. 8A and C, respectively), the retention times of the α-helical analogues decreased by an average of ∼10 min; in contrast, the retention time decrease for P_D and P_L was 7.5 and 8 min, respectively. Such results, where P_D and P_L exhibit a different response to temperature variation relative to the other peptides, are similar to those observed at pH 2.0 (Fig. 7).

4. Conclusions

In the present study, we have demonstrated how variations in column packing, mobile phase conditions and temperature allow useful manipulation of elution profiles of amphipathic α-helical peptides at both pHs 2.0 and 7.0. In particular, the perchlorate anion (ClO_4^-) has proved to be an excellent hydrophilic ion-pairing reagent where there is a net positive charge on the peptide. In addition, it can be used as an ion-pairing reagent in the pH range of pHs 2.0–7.0, unlike acidic anionic ion-pairing reagents such as TFA. Coupled with the different selectivities observed for peptide separations achievable with different C_8 packings and/or temperature (the latter achievable via conformational differences between peptides), our observations are applicable to the rational development of separation/optimization protocols for peptide/proteomic applications.

Acknowledgements

This work was supported by an NIH grant (RO1 GM 61855) to R.S. Hodges.

References

[1] J.P. Segrest, H. De Loof, J.G. Dohlman, C.G. Brouilette, G.M. Anantharamaiah, Proteins: Struct. Funct. Genet. 8 (1990) 103.
[2] J.L. Cornette, K.B. Cease, H. Margalit, J.L. Spouge, J.A. Berzofsky, C.D. DeLisi, J. Mol. Biol. 195 (1987) 659.
[3] C.T. Mant, N.E. Zhou, R.S. Hodges, in: R.E. Epand (Ed.), The Amphipathic Helix, CRC Press, Boca Raton, FL, 1993, p. 39.
[4] R.S. Hodges, Biochem. Cell Biol. 74 (1996) 133.
[5] Y. Chen, C.T. Mant, R.S. Hodges, J. Pept. Res. 59 (2002) 18.
[6] S.E. Blondelle, K. Lohner, M. Aguilar, Biochim. Biophys. Acta 1462 (1999) 89.
[7] R.M. Epand, H.J. Vogel, Biochim. Biophys. Acta 1462 (1999) 11.
[8] B. Bechinger, J. Membr. Biol. 156 (1997) 197.
[9] M. Wu, R.E.W. Hancock, J. Biol. Chem. 274 (1999) 29.
[10] C.T. Mant, R.S. Hodges (Eds.), High-Performance Liquid Chromatography of Peptides and Proteins: Separation, Analysis and Conformation, CRC Press, Boca Raton, FL, 1991.
[11] C.T. Mant, R.S. Hodges, in: K.M. Gooding, F.E. Regnier (Eds.), HPLC of Biological Macromolecules, Marcel Dekker, New York, NY, 2002, p. 433.
[12] N.E. Zhou, C.T. Mant, R.S. Hodges, Pept. Res. 3 (1990) 8.
[13] S.E. Blondelle, K. Büttner, R.A. Houghten, J. Chromatogr. 625 (1992) 199.
[14] R.S. Hodges, B.-Y. Zhu, N.E. Zhou, C.T. Mant, J. Chromatogr. A 676 (1994) 3.
[15] A.W. Purcell, M.I. Aguilar, R.E.W. Wettenhall, M.T.W. Hearn, Pept. Res. 8 (1995) 160.
[16] S.E. Blondelle, J.M. Ostresh, R.A. Houghten, Biophys. J. 68 (1995) 351.
[17] D.L. Steer, P.E. Thompson, S.E. Blondelle, R.A. Houghten, M.I. Aguilar, J. Pept. Res. 51 (1998) 401.
[18] T.J. Sereda, C.T. Mant, F.D. Sönnichsen, R.S. Hodges, J. Chromatogr. A 676 (1994) 139.
[19] C.T. Mant, R.S. Hodges, J. Chromatogr. A 972 (2002) 45.
[20] C.T. Mant, R.S. Hodges, J. Chromatogr. A 972 (2002) 61.
[21] T.J. Sereda, C.T. Mant, R.S. Hodges, J. Chromatogr. A 695 (1995) 205.
[22] Y. Chen, C.T. Mant, R.S. Hodges, J. Chromatogr. A 1010 (2003) 45.
[23] J.W. Nelson, N.R. Kallenbach, Biochemistry 28 (1989) 5256.
[24] T.M. Cooper, R.W. Woody, Biopolymers 30 (1990) 657.
[25] F.D. Sönnichsen, J.E. Van Eyk, R.S. Hodges, B.D. Sykes, Biochemistry 31 (1992) 8790.
[26] N.E. Zhou, B.-Y. Zhu, B.D. Sykes, R.S. Hodges, J. Am. Chem. Soc. 114 (1992) 4321.
[27] N.E. Zhou, C.M. Kay, B.D. Sykes, R.S. Hodges, Biochemistry 32 (1993) 6190.
[28] N.E. Zhou, C.M. Kay, R.S. Hodges, J. Mol. Biol. 237 (1994) 500.
[29] N.E. Zhou, O.D. Monera, C.M. Kay, R.S. Hodges, Protein Pept. Lett. 1 (1994) 114.
[30] O.D. Monera, T.J. Sereda, N.E. Zhou, C.M. Kay, R.S. Hodges, J. Pept. Sci. 1 (1995) 319.
[31] P.Y. Chou, G.D. Fasman, Biochemistry 13 (1974) 222.
[32] J.M. Scholtz, H. Qian, V.H. Robbins, R.L. Baldwin, Biochemistry 32 (1993) 9668.
[33] K.R. Shoemaker, P.S. Kim, E.J. York, J.M. Stewart, R.L. Baldwin, Nature 326 (1987) 563.
[34] M.I. Aguilar, S. Mougos, J. Boublik, J. Rivier, M.T.W. Hearn, J. Chromatogr. A 646 (1993) 53.
[35] S. Rothemund, M. Beyermann, E. Krause, G. Krause, M. Bienert, R.S. Hodges, B.D. Sykes, F.D. Sönnichsen, Biochemistry 34 (1995) 12954.
[36] S. Rothemund, E. Krause, M. Beyermann, M. Dathe, M. Bienert, R.S. Hodges, B.D. Sykes, F.D. Sönnichsen, Pept. Res. 9 (1996) 79.
[37] E. Krause, M. Bienert, P. Schmieder, H. Wenschuh, J. Am. Chem. Soc. 122 (2000) 4865.
[38] T.J. Sereda, C.T. Mant, A.M. Quinn, R.S. Hodges, J. Chromatogr. 646 (1993) 17.
[39] H. Gaertner, A. Puigserver, J. Chromatogr. 350 (1985) 279.
[40] D. Guo, C.T. Mant, R.S. Hodges, J. Chromatogr. 386 (1987) 205.
[41] Cs. Horváth, W. Melander, I. Molnár, J. Chromatogr. 125 (1976) 129.
[42] Cs. Horváth, W. Melander, I. Molnár, P. Molnár, Anal. Chem. 49 (1977) 2295.
[43] P.T. Kissinger, Anal. Chem. 49 (1977) 883.
[44] J.C. Kraak, K.M. Jonker, J.F.K. Huber, J. Chromatogr. 142 (1977) 671.
[45] J.L.M. van de Venne, J.L.H.M. Hendrikx, R.S. Deelder, J. Chromatogr. 167 (1978) 1.
[46] J.L. Meek, Proc. Natl. Acad. Sci. U.S.A. 77 (1980) 1632.
[47] D. Guo, C.T. Mant, A.K. Taneja, J.M.R. Parker, R.S. Hodges, J. Chromatogr. 359 (1986) 499.
[48] C.T. Mant, R.S. Hodges, Chromatographia 24 (1987) 805.
[49] R.H. Snider, C.F. Moore, E.S. Nylen, K.L. Becker, Horm. Metab. Res. 20 (1988) 254.
[50] T.J. Sereda, C.T. Mant, R.S. Hodges, J. Chromatogr. A 776 (1997) 153.
[51] B.-Y. Zhu, C.T. Mant, R.S. Hodges, J. Chromatogr. 594 (1992) 75.
[52] K. Titani, T. Sasagawa, K. Resing, K. Walsh, Anal. Biochem. 123 (1982) 408.
[53] G.E. Tarr, J.W. Crabb, Anal. Biochem. 131 (1983) 99.
[54] L.R. Gurley, D.A. Prentice, J.G. Valdez, W.D. Spall, Anal. Biochem. 131 (1983) 465.
[55] W.G. Burton, K.D. Nugent, T.K. Slattery, B.R. Summers, L.R. Snyder, J. Chromatogr. 443 (1988) 363.
[56] N.E. Zhou, C.T. Mant, J.J. Kirkland, R.S. Hodges, J. Chromatogr. 548 (1991) 179.
[57] B.A. Marchylo, D.W. Hatcher, J.E. Kruger, J.J. Kirkland, Cereal Chem. 69 (1992) 371.
[58] B.E. Boyes, D.G. Walker, J. Chromatogr. A 691 (1995) 337.
[59] J.J. Kirkland, J.L. Glajch, R.D. Farlee, Anal. Chem. 61 (1989) 2.
[60] J.L. Glajch, J.J. Kirkland, LC·GC 8 (1990) 140.
[61] B.E. Boyes, J.J. Kirkland, Pept. Res. 6 (1993) 249.
[62] J.J. Kirkland, J.W. Henderson, J.J. De Stefano, M.A. van Straten, H.A. Claessens, J. Chromatogr. A 762 (1997) 97.
[63] J.J. Kirkland, M.A. van Straten, H.A. Claessens, J. Chromatogr. A 797 (1998) 111.
[64] W.S. Hancock, R.C. Chloupek, J.J. Kirkland, L.R. Snyder, J. Chromatogr. A 686 (1994) 31.
[65] R.C. Chloupek, B.A. Hancock, B.A. Marchylo, J.J. Kirkland, B.E. Boyes, L.R. Snyder, J. Chromatogr. A 686 (1994) 45.
[66] C.T. Mant, L.H. Kondejewski, P.J. Cachia, O.D. Monera, R.S. Hodges, Methods Enzymol. 289 (1997) 426.
[67] F.D. Antia, Cs. Horváth, J. Chromatogr. 435 (1988) 1.
[68] J.W. Li, P.W. Carr, Anal. Chem. 69 (1997) 2202.
[69] J.W. Li, P.W. Carr, Anal. Chem. 69 (1997) 2550.
[70] C.T. Mant, Y. Chen, R.S. Hodges, J. Chromatogr. A 1009 (2003) 29.
[71] C.T. Mant, B. Tripet, R.S. Hodges, J. Chromatogr. A 1009 (2003) 45.